Available online at www.sciencedirect.com
SCIENCE DIRECT
Solid State Communications 137 (2006) 182–186
solid state communications
www.elsevier.com/locate/ssc

# Growth of vertically aligned single crystal ZnO nanotubes by plasma-molecular beam epitaxy

H.W. Liang [a,*], Y.M. Lu [b], D.Z. Shen [b], B.H. Li [b], Z.Z. Zhang [b], C.X. Shan [c], J.Y. Zhang [b], X.W. Fan [b], G.T. Du [a]

[a] State Key Laboratory for Materials Modification by Laser, Ion, Electron Beams, Department of Physics, Dalian University of Technology, 2-Linggong Road, Dalian 116024, People's of Republic China
[b] Laboratory of Excited State Processes, Chang Chun Institute of Optics, Fine Mechanics and Physics, Chinese Academy of Sciences, 16-Dongnanhu Road, Changchun 130033, People's of Republic China
[c] Department of Physics, Chinese University of Hong Kong, Shatin, New Territory, Hong Kong

Received 27 August 2005; accepted 11 November 2005 by H. Akai
Available online 5 December 2005

**Abstract**

Highly oriented and vertically aligned single crystalline ZnO nanotubes were fabricated on $Al_2O_3$ (0001) substrates by plasma-molecular beam epitaxy without employing any external metal catalysts or templates. Field emission scanning electron microscope images indicate that the regularly aligned ZnO nanotubes with uniform size distribution were obtained. The chimney-like single crystal ZnO nanotube was confirmed by the transmission electron microscope and selected area electron diffraction pattern of the single nanotube. The formation mechanism of the nanotubes was also described briefly.


*PACS:* 52.40.Mj; 81.05.Dz; 81.15.Hi; 61.46.+w

*Keywords:* A. ZnO nanotubes; A. O-plasma; B. Plasma-molecular beam epitaxy; D. Polar and non-polar planes

## 1. Introduction

Since Iijima first reported carbon nanotubes in 1991, great interest in such tubular materials have arisen due to their peculiar features such as low dimension, large surface to volume ratio and high anisotropy with new physical, chemical properties [1–3]. They find potential applications in scanning microscopes and sensors [4], field emission devices [5], biological probes [6] and nanoelectronics [7]. The production of nanotubes with high order is one of the most important issues in the nanotubes society [3]. ZnO is a wurtzite-structured II–VI compound with a band gap of 3.37 eV. It has many applications, such as optically transparent conducting layers, photovoltaic devices and gas sensors [8]. Because of its large exciton binding energy (60 meV), which allows efficient light emission from excitonic recombination at room temperature. ZnO is also a promise candidate in blue and ultraviolet light-emitting devices [9]. Preliminary progresses have been achieved in the research of ZnO one-dimensional (1D) structures, such as, nanowires [10] and nanowalls [11], and nanorods [12] etc. As a member of the 1D nanostructure, ZnO nanotubes were usually obtained by using thermal evaporation of the Zn core of the Zn/ZnO nanocables formed by the reduction of ZnS powder under hydrogen treatment at high temperatures [13], or by directly evaporating a mixture of Zn/ZnO powder [14]. More recently, well-aligned ZnO tubes were also fabricated by metalorganic chemical vapor deposition, but the size is beyond nanoscale [15].

In this paper, catalyst-free-fabrication of highly oriented ZnO nanotubes on $Al_2O_3$ substrate by plasma-assisted molecular beam epitaxy is reported. Transmission electron microscopy (TEM) measurement reveals that the obtained tubes are single crystal having wurtzite structure in nature. The possible formation mechanism of nanotubes will be explained by the difference in stability between the polar and non-polar planes in this paper.

* Corresponding author. Tel.: +86 411 84707865.
*E-mail address:* hwliang@dlut.edu.cn (H.W. Liang).

0038-1098/$ - see front matter © 2005 Elsevier Ltd. All rights reserved.
doi:10.1016/j.ssc.2005.11.028

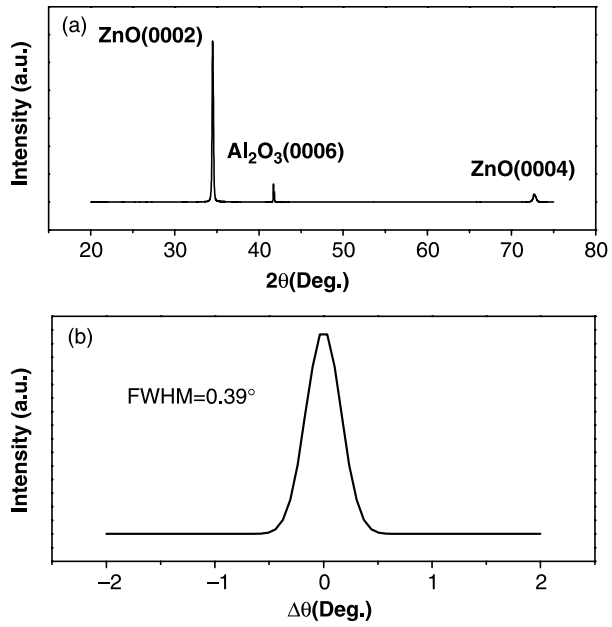


Fig. 1. (a) X-ray diffraction pattern and (b) X-ray rocking curves of ZnO nanotubes.

## 2. Experiment

$Al_2O_3$ (0001) substrates with a well-polished *c*-plane were cleaned in acetone followed by ethanol in an ultrasonic bath to remove dust and surface contamination. They were then etched in hot $H_2SO_4$:$H_3PO_4$ = 3:1 solution (160 °C) for 10 min, rinsed in de-ionized water (18.2 MΩ $cm^{-1}$) and dried with high-purity nitrogen. The chemically treated substrates were sent into the growth chamber ($\leq 1\times10^{-7}$ Pa) by an indium solder on a molybdenum holder to receive a 30-min heating treatment at 800 °C. Elemental zinc of 99.9999% purity and oxygen of 99.999% purity were used as source materials. Zinc was evaporated by a Knudsen effusion cell, and oxygen was activated by an RF plasma source (13.56 MHz) at a fixed power of 300 W, provided by Oxford Applied Research. An electrostatic ion trap (EIT) operating at 500 V was used to separate ions from the O-plasma during the growth process. When the EIT is turned on, only neutral atoms or molecules are allowed to reach the substrate, while both ions and neutral atoms can enter when off. Before growth, the substrate was treated in O-plasma at 550 °C for 40 min while the EIT was off. Afterwards the EIT was turned on and a thin ZnO buffer layer (~3 nm) was grown, which was then treated by O-plasma for 30 min with the EIT being turned off to form the ring-like ZnO template. ZnO nanotubes were then grown on this template for 2 h while the EIT was on. The partial pressures of Zn and O in the growth process were fixed at $4\times10^{-4}$ and $6\times10^{-3}$ Pa, respectively.

The crystal structure of the prepared samples was characterized by X-ray diffractometer (Rigaku O/max-RA) and double crystal diffractometer (D/Max 2400). Surface morphology was accessed by a field emission scanning electron microscopy (FE-SEM) and an atomic force microscope (AFM) working in the tapping mode. In order to confirm further the tubular and single crystalline structure of as-grown ZnO, transmission electron microscope (TEM) measurements were performed.

## 3. Results and discussion

Fig. 1(a) shows the X-ray diffraction (XRD) pattern and Fig. 1(b) shows the X-ray rocking curve (XRC) for the grown samples. In Fig. 1(a), besides the $Al_2O_3$ (0006) peak located

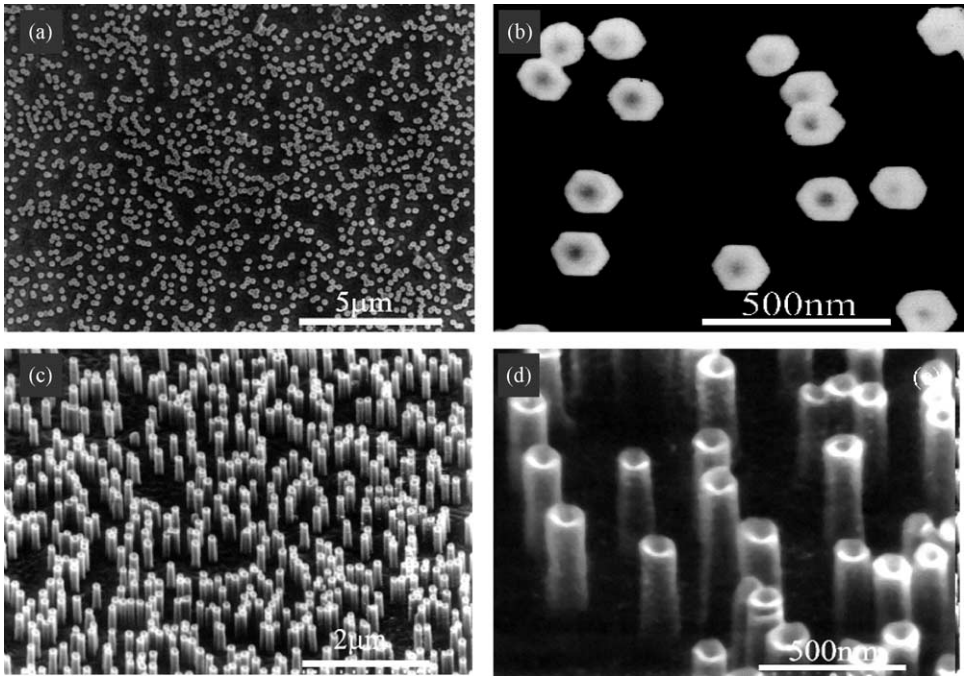


Fig. 2. FE-SEM images of the ZnO nanotubes. (a) Low-magnification top-view. (b) High-magnification top-view. (c) Low-magnification 45° side view. (d) High-magnification 45° side view.


Fig. 3. The TEM image of a single ZnO nanotube. The inset is the selected area electron diffraction pattern.

at 41.71°, only the diffraction peaks of ZnO (0002) and (0004) were observed at 34.46 and 73.69°, respectively. It indicates that the ZnO sample has the wurtzite structure with its *c*-axis perpendicular to the *c*-plane of the substrates. The surface morphology of the sample analyzed by FE-SEM is shown in Fig. 2(a). It shows a discontinuous structure with homogeneous distribution with the density of about $7\times10^8$ cm$^{-2}$. Fig. 2(b) is a high-magnification image, which clearly shows a regular hexagonal structure. Figs. 2(c) and (d) are side-views at 45° that show the ZnO tubular structures are regularly arranged and well aligned. In order to further confirm the tubular structure, the single nanotube was analyzed by TEM, as seen in Fig. 3. It is clearly shown that the single nanotube is the chimney-like top open tubular structure. The length of the single nanotubes is about 480 nm. The top diameter and wall thickness of the nanotube are about 70 and 20 nm, respectively. While the bottom diameter and wall thickness is about 90 and 33 nm. The inset of Fig. 3 is the selected area electron diffraction (SAED) pattern of the nanotube. The sharp diffraction spots in the SAED pattern indicate the single crystal nature of the nanotube.

From the energy depressive X-ray data equipped in the SEM chamber, the stoichiometric ratio of Zn and O atoms is about 1:1. There are no impurities in the sample, which helps to exclude the usual catalyst-assisted growth mechanism of nanotubes. It was found that the tubular structures could only form after the substrate is treated by O-plasma. To explain the effect of O-plasma treatment, AFM is used to study the $Al_2O_3$ substrate surface. The AFM image in Fig. 4(a) shows that the untreated substrate has a smooth surface with a step height of 0.2 nm, which is close to 1/6 of the $Al_2O_3$ lattice constant along the *c*-axis direction. Fig. 4(b) exhibits the surface morphology of the substrate treated by O-plasma at 550 °C for 30 min. The increase in surface roughness and formation of uniformly distributed pits with size around 80 nm can be seen clearly. These pits are due to surface damage induced by O-plasma treatment. To study the influence of plasma in the initial stage of growth, 3-nm-thick ZnO layers were grown on the both substrates treated and untreated by O-plasma, and their surface morphologies are shown in Fig. 5. In Fig. 5(a), many ZnO islands can be seen on the plasma-treated substrate, and the island size is almost as large as the pit size. The lattice mismatch between ZnO and $Al_2O_3$ is as high as 18% in *c*-plane, which results in a large number of defects and dislocations in the ZnO film. Further two-dimensional growth is very difficult because ZnO atoms can nucleate easily on these defects. Thus, ZnO islands are formed in the pits by atomic migration and diffusion on the plasma-treated substrate surface. If these islands are treated by plasma for 30 min, many ring-like ZnO structures are formed on the substrate surface, as seen in Fig. 5(b). The size of these ring-like structures is the same as that of the nanotubes but slightly greater than that of the ZnO islands. For comparison, Fig. 5(c) shows the surface morphology of ZnO film with 3 nm thickness grown on the untreated substrate. A smooth surface without distinct islands or ring-like structures is observed, which indicates that the plasma process plays a key role in forming nanotubes. For the plasma-treated substrates, the pits act as the nucleation sites for

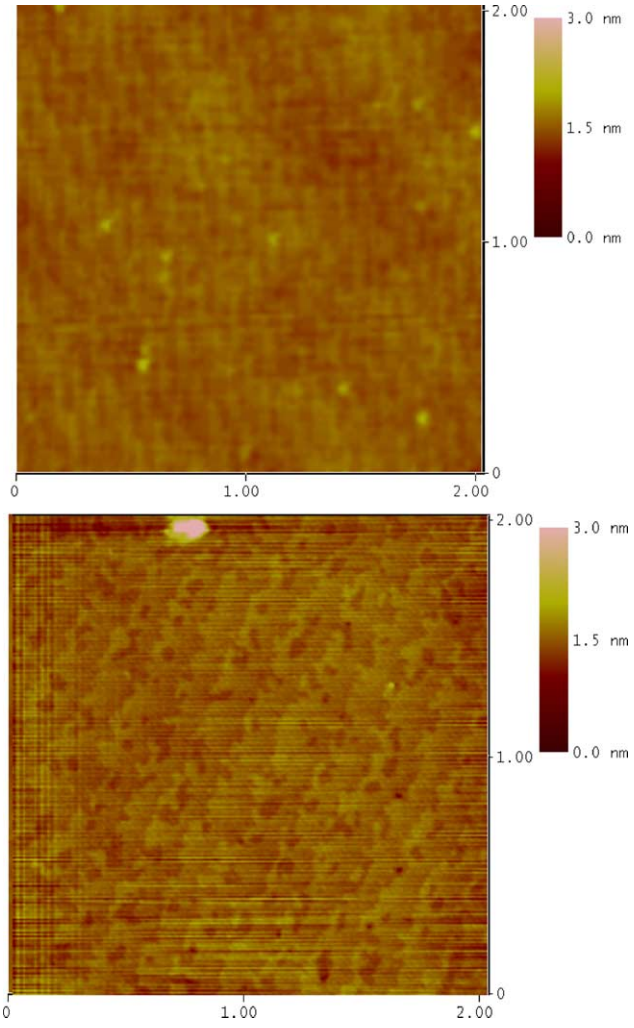


Fig. 4. AFM images of as-degreased (a) and O-plasma treated $Al_2O_3$ substrates (b).

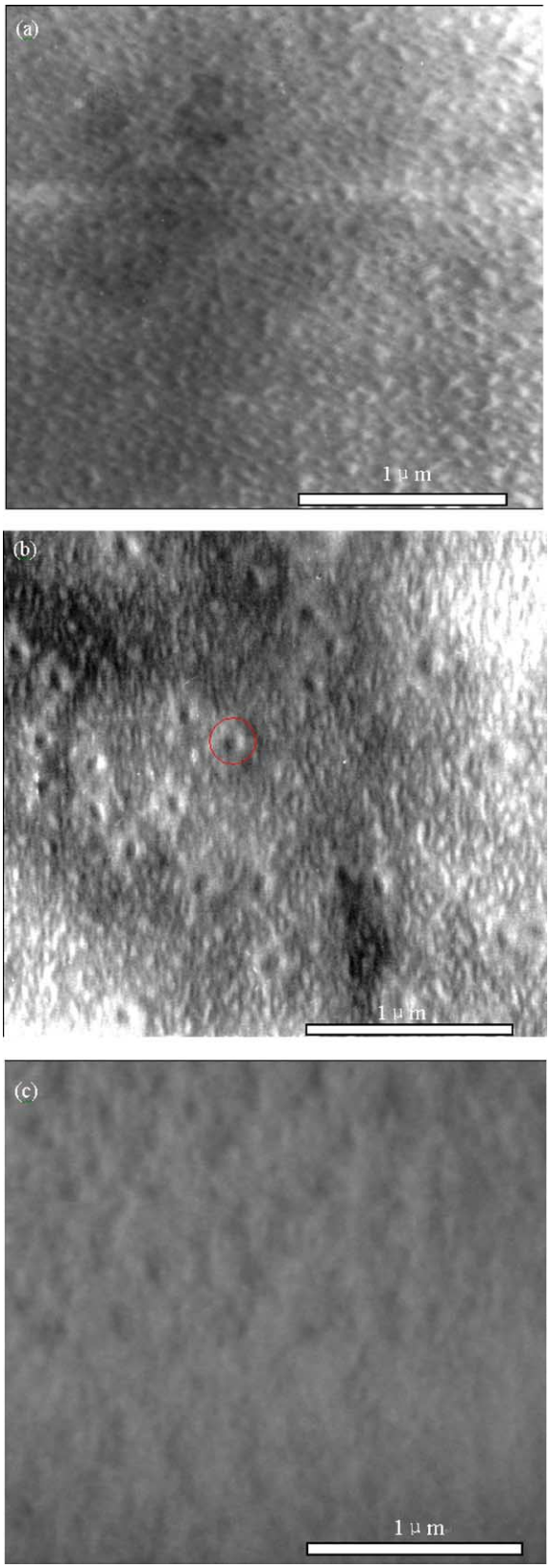


Fig. 5. (a) FE-SEM images of the as-grown 3 nm thick ZnO films. (b) The ZnO film treated by O-plasma for 30 min. The red circle is the guide for eyes. (c) ZnO films grown on untreated $Al_2O_3$ substrate.

the island structures. Under the action of plasma, these islands reconstruct to ring-like structures by the diffusion of the surface atoms. It is reasonable to consider that the ring-like structure acts as template for the formation of nanotubes. Further growth on these rings is homo-epitaxial and the smaller mismatch lowers the formation energy. Therefore, successive atoms can be deposited easily on these rings to form nanotubes.

To further understand the mechanism responsible for the action of plasma on ZnO ring-like structures, it is necessary to study the stability of the different ZnO faces. ZnO has a hexagonal structure with space group $P6_{3mc}$. The surfaces of its hexagonal column consist of a basal polar O-terminated $(000\bar{1})$ plane, a top polar Zn-terminated (0001) plane, and six low-index non-polar $(11\bar{2}0)$ planes. Since the polar surface is less stable than the non-polar surface, the inherent asymmetry and anisotropy allow for the preferential growth of the crystal along the *c*-axis direction [16]. This means that under external influences, ZnO atoms tend to escape from the polar surface. By this way, Vayssiers et al., had successfully prepared aligned ZnO micron tubes by aging the micron column [16]. In this work, ZnO nanotubes with the preferred orientation of ZnO (0002) are grown on the *c*-plane of $Al_2O_3$ substrate, and the ZnO surfaces comprise the metastable polar planes and the stable non-polar planes. When the ZnO islands are processed in O-plasma, the atoms on the polar surface will migrate to the non-polar surfaces, which causes the islands to evolve into ring structures with slightly increased diameter. Tubular structures were then formed employing the rings as templates.

The diameter of the ZnO nanotubes can be controlled by the growth condition, such as the thickness of the initial ZnO film and the treatment time of the O-plasma. Moreover, the nanotubes show very good optical properties and the details of which will be published elsewhere. What interests us lies in that the formation method in this study may open one new route to the preparation of tubular structures.

## 4. Conclusion

In this paper, vertical aligned ZnO nanotubes were grown by plasma-assisted MBE. TEM measurement reveals that the tubes are single crystal with hexagonal wurtzite structure. The formation mechanism of the tubes was also studied. The ring-like structure induced by the O-plasma treatment was considered as the template for the formation of the tubes. The successful growth of well-aligned ZnO nanotubes assisted by plasma treatment may provide a new route to the synthesis of tubular structures in nanometer scale.

## Acknowledgements

This work is supported by the '863' High Technology Research Program in China under Grant No 2001AA31112, the Key Project of the National Natural Science Foundation of China under Grant No 60336020, the Innovation Project of Chinese Academy of Sciences, the National Natural Science Foundation of China under Grant No 60278031, No 60176003 and No 60376009.

## References

[1] S. Iijima, Nature 354 (1991) 56.
[2] A. Hamwi, H. Alvergnat, S. Bonnamy, F. Beguin, Carbon 35 (1997) 723.
[3] K.-T. Lau, D. Hui, Compos Part B 33 (2002) 263.
[4] R. Service, Science 281 (1998) 940.
[5] S. Fan, M.G. Chapline, N.R. Franklin, T.W. Tombler, A.M. Cassell, H. Dai, Science 283 (1999) 512.
[6] G.I. Dovbeshko, O.P. Repnytska, E.D. Obraztsova, Y.V. Shtogun, Chem. Phys. Lett. 372 (2003) 432.
[7] S.J. Tans, R.M. Verschueren, C. Dekker, Nature 393 (1998) 49.
[8] A. Uedono, T. Koida, A. Tsukazaki, M. Kawasaki, Z.Q. Chen, S.F. Chichibu, H. Koinuma, J. Appl. Phys. 93 (2003) 2481.
[9] Z.K. Tang, G.K.L. Wong, P. Yu, M. Kawasaki, A. Ohtomo, H. Koinuma, Y. Segawa, Appl. Phys. Lett. 72 (1998) 3270.
[10] S.H. Jo, J.Y. Lao, Z.F. Ren, R.A. Farrer, T. Baldacchini, J.T. Fourkas, Appl. Phys. Lett. 83 (2003) 4821.
[11] H.T. Ng, J. Li, M.K. Smith, P. Nguyen, A. Cassell, J. Han, M. Meyyappan, Science 300 (2003) 1249.
[12] J.J. Wu, S.C. Liu, Adv. Mater. 14 (2002) 215.
[13] J.Q. Hu, Q. Li, X.M. Meng, C.S. Lee, S.T. Lee, Chem. Mater. 15 (2003) 305.
[14] Y.J. Xing, Z.H. Xi, Z.Q. Xue, X.D. Zhang, J.H. Song, R.M. Wang, J. Xu, Y. Song, S.L. Zhang, D.P. Yu, Appl. Phys. Lett. 83 (2003) 1689.
[15] B.P. Zhang, N.T. Binh, K. Wakatsuki, Y. Segawa, Y. Yamada, N. Usami, M. Kawasaki, H. Koinuma, Appl. Phys. Lett. 84 (2004) 4098.
[16] L. Vayssieres, K. Keis, A. Hagfeldt, S.E. Lindquist, Chem. Mater. 13 (2001) 4395.